

Critical examination of isotope shift and fine structure measurements for optical transitions in ${}^6,{}^7\text{Li}^1$

George A. Noble and William A. van Wijngaarden

Abstract: Precise isotope shift and fine structure measurements are critically reviewed. Each experiment was checked for whether the data found for different transitions yielded consistent values for the difference in mean-square nuclear charge radius Δr^2 of ${}^6,{}^7\text{Li}$. Experiments that passed this test found $\Delta r^2 = 0.735 \pm 0.036$, 0.755 ± 0.023 , and $0.739 \pm 0.013 \text{ fm}^2$ by studying the $\text{Li}^+ 1s2s {}^3\text{S} \rightarrow 1s2p {}^3\text{P}$ transition, the Li D lines and the $\text{Li } 2S_{1/2} \rightarrow 3S_{1/2}$ transition, respectively. These data determine the difference in mean-square nuclear charge radius 25 times more accurately than electron scattering. Similarly, averaging the fine structure data from the same experiments gives $62\,678.75 \pm 0.55 \text{ MHz}$ for the ${}^7\text{Li}^+ 1s2p {}^3\text{P}_{1-2}$ interval, in good agreement with theory. The results for the ${}^6,{}^7\text{Li } 2\text{P}$ fine structure intervals, $10\,052.954 \pm 0.049$ and $10\,053.154 \pm 0.040 \text{ MHz}$, exceed computed values by 2 MHz and yield a splitting isotope shift, which is nearly a factor of 2 lower than a theoretical estimate.

PACS Nos: 31.30Gs, 32.10.Fn

Résumé : Nous passons en revue serrée les déplacements isotopiques et les mesures de structure fine dans ${}^6,{}^7\text{Li}$. Chaque expérience a été vérifiée pour voir si les données pour les différentes transitions donnaient des valeurs cohérentes pour le rayon au carré de la charge nucléaire relative Δr^2 . Les expériences qui ont passé ce test donnent $\Delta r^2 = 0,735 \pm 0,036$, $0,755 \pm 0,023$ et $0,739 \pm 0,013 \text{ fm}^2$ en étudiant respectivement la transition $\text{Li}^+ 1s2s {}^3\text{S} \rightarrow 1s2p {}^3\text{P}$, les lignes Li D et la transition $\text{Li } 2S_{1/2} \rightarrow 3S_{1/2}$. Ces données permettent de déterminer le rayon de charge nucléaire relatif avec une précision 25 fois meilleure qu'avec la diffusion d'électrons. De façon similaire, prenant la moyenne des valeurs les plus fiables des données de structure fine, nous obtenons $62\,678,75 \pm 0,55 \text{ MHz}$ pour l'intervalle ${}^7\text{Li } 1s2p {}^3\text{P}_{1-2}$, en bon accord avec la théorie. Les valeurs d'intervalle de structure fine pour le ${}^6,{}^7\text{Li } 2\text{P}$, $10\,052,954 \pm 0,049$ et $10\,053 \pm 0,040 \text{ MHz}$ dépassent les valeurs calculées par 2 MHz et donnent un déplacement isotopique qui est pratiquement 2 fois plus faible que l'estimé théorique.

[Traduit par la Rédaction]

1. Introduction

The most accurate determinations of the charge radii of light nuclei are obtained by measuring isotope shifts of optical transitions and using high-precision theory to extract the effect of the finite nuclear size [1–4]. Advances in high-precision theory using the so called Hylleraas basis set to obtain eigenenergies corresponding to the nonrelativistic Hamiltonian are well documented [1, 5]. The corresponding wave functions can be used to perturbatively evaluate relativistic, QED, and hyperfine effects. One is left with the contribution due to the finite size of the nucleus given by,

$$E_{\text{Nuc}} = \frac{2\pi}{3} Z e^2 r^2 \left\langle \sum_i \delta(r_i) \right\rangle \quad (1)$$

where r is the root-mean-square nuclear charge radius, Z is the number of protons, and e is the proton charge. The sum-

mation term equals the expectation value of the electron density at the nucleus where i is summed over all electrons of the atom [1]. The difference in mean-square nuclear charge radius Δr^2 between two isotopes such as ${}^6\text{Li}$ and ${}^7\text{Li}$ is defined by,

$$\Delta r^2 = r^2({}^6\text{Li}) - r^2({}^7\text{Li}) \quad (2)$$

can be found using

$$\Delta r^2 = \frac{I_{jk} - E_{jk}}{C_{jk}} \quad (3)$$

Here, I_{jk} is the measured isotope shift for a transition between states j and k , E_{jk} is the calculated isotope shift excluding the effect of the nuclear size called the mass shift, and C_{jk} is the shift dependence on the nuclear size defined using (1).

In the case of lithium, isotope shift data have been obtained by a number of experiments for the $\text{Li}^+ 1s2s$

Received 10 October 2008. Accepted 22 January 2009. Published on the NRC Research Press Web site at cjp.nrc.ca on 9 September 2009.

G.A. Noble and W.A. vanWijngaarden.² Dept. of Physics, York University, Petrie Bldg, 4700 Keele St, Toronto, ON M3J 1P3, Canada.

¹This paper was presented at the International Conference on Precision Physics of Simple Atomic Systems, held at University of Windsor, Windsor, Ontario, Canada on 21–26 July 2008.

²Corresponding author (e-mail: wlaser@yorku.ca).

Table 1. Calculated mass shift and dependence on nuclear size.

Transition	Mass shift E_{jk} (MHz)	C_{jk} (MHz/fm ²)	Ref.
$\text{Li}^+ 2\ ^3\text{S}_1 \rightarrow 2\ ^3\text{P}_0$	$34\ 740.17 \pm 0.03$	9.705	[1]
$\text{Li}^+ 2\ ^3\text{S}_1 \rightarrow 2\ ^3\text{P}_1$	$34\ 739.87 \pm 0.03$	9.705	[1]
$\text{Li}^+ 2\ ^3\text{S}_1 \rightarrow 2\ ^3\text{P}_2$	$34\ 742.71 \pm 0.03$	9.705	[1]
$\text{Li } 2\ ^2\text{S}_{1/2} \rightarrow 2\ ^3\text{P}_{1/2}$	$10\ 532.17 \pm 0.07$	2.457	[1]
	$10\ 532.111 \pm 0.006$		[7]
$\text{Li } 2\ ^2\text{S}_{1/2} \rightarrow 2\ ^3\text{P}_{3/2}$	$10\ 532.57 \pm 0.07$	2.457	[1]
	$10\ 532.506 \pm 0.006$		[7]
$\text{Li } 2\ ^2\text{S}_{1/2} \rightarrow 3\ ^2\text{S}_{1/2}$	$11\ 453.010 \pm 0.056$	1.5661	[2]
	$11\ 452.822 \pm 0.002$	1.5732	[8]
	$11\ 452.821 \pm 0.002$		[7]

$^3\text{S}_1 \rightarrow 1\text{s}2\text{p } ^3\text{P}_{0,1,2}$ transitions, the Li D1 and D2 lines, as well as the for the two-photon transition $\text{Li } 2\ ^2\text{S}_{1/2} \rightarrow 3\ ^2\text{S}_{1/2}$. These transitions occur at optical wavelengths where narrow line width lasers facilitate precision measurements. Table 1 lists values of E_{jk} and C_{jk} computed for these transitions. The initial calculations by Drake and collaborators [6] were recently refined to include high-order relativistic effects [7]. Their latest value for the mass shift is nearly identical with that found previously by the independent theoretical group of Puchalski for the $\text{Li } 2\ ^2\text{S}_{1/2} \rightarrow 3\ ^2\text{S}_{1/2}$ transition [8].

This paper is organized as follows. First, experiments reporting isotope shift and fine structure splitting data having accuracies of better than 1 MHz are reviewed. Most experiments measured isotope shifts of multiple transitions. Inconsistent results of the field shift $I_{jk} - E_{jk}$ and in turn Δr^2 indicate that either the experiment or the theoretically computed mass shift is in error. The calculated mass shifts of the D1 and D2 lines differ by 0.395 MHz. Hence, inconsistencies of the field shift >1 MHz are likely due to underestimating the experimental uncertainty. Data found by experiments that yielded consistent results are averaged to obtain the most reliable isotope shifts and fine structure splittings.

2. Review of experimental work

2.1. $\text{Li}^+ 1\text{s}2\text{s } ^3\text{S} \rightarrow 1\text{s}2\text{p } ^3\text{P}$ transition

The $\text{Li}^+ 1\text{s}2\text{s } ^3\text{S}$ state has a lifetime of nearly one minute, which is sufficient for laser spectroscopy. Metastable lithium ions are generated by first heating lithium in an oven to a temperature of about 500 °C. The atoms are then bombarded with an electron beam. The resulting ions are collimated by an electrostatic lens and accelerated. Typical Li^+ currents of 1 μA can be generated where about 0.1% of the ions occupy the metastable state [9].

The groups of Rong et al. [10] and Riis et al. [11] each used two ring dye lasers having a line width of about 1 MHz to determine absolute frequencies of transitions. Isotope shift and fine structure splittings were obtained by taking differences of the various transition frequencies. The laser heterodyne (LH) experiment of Rong et al. [10] locked one laser to an iodine transition using the saturated absorption technique [12]. The second laser perpendicularly intersected a 300 eV Li^+ beam and was retro-reflected by a mirror. Fluorescence, produced by the radiative decay of

the $1\text{s}2\text{p } ^3\text{P}$ state, was detected by a photomultiplier as the laser frequency was scanned across the resonance. Each transition was observed to consist of a 200 MHz FWHM Lamb dip superimposed on a 2 GHz FWHM Doppler-broadened line shape. The Doppler background was removed by subtracting data collected with the retro-reflected laser beam blocked. The second laser was locked to the center of the Lamb dip. The frequency difference between the two dye lasers was found by focussing part of each laser beam onto a fast photodiode that could detect frequencies of up to 12.5 GHz. Frequency intervals up to 150 GHz were found by measuring multiple smaller intervals using intermediate iodine lines to lock the two dye lasers. The uncertainty listed in Table 2 for the fine structure interval equals three times the standard deviation of the observations about the average value.

The experiment of Riis et al. [11] used two lasers to excite an ion beam (LIB). A saturation spectroscopy signal was obtained by having the two laser beams propagate parallel and antiparallel with a 100 keV metastable Li^+ beam. The dye laser copropagating with the ion beam was Doppler-tuned into resonance with one of the $^6,7\text{Li}^+ 1\text{s}2\text{s } ^3\text{S}_1 \rightarrow 1\text{s}2\text{p } ^3\text{P}_{0,1,2}$ transitions by slightly varying the ion acceleration voltage. The second dye laser, counter-propagating with the ions, was scanned across the resonance using an acousto-optic modulator (AOM). A photomultiplier observed a fluorescence signal consisting of a 25 MHz FWHM Lamb dip superimposed on a 100 MHz FWHM Doppler broadened peak. The Lamb dip signal was isolated by subtracting the Doppler-broadened signal obtained when the first dye laser was blocked. Absolute frequencies of both dye lasers were found using a wavemeter and a Fabry–Perot etalon, whose length was locked using an iodine stabilized HeNe laser. The fine structure of the $1\text{s}2\text{p } ^3\text{P}_{1-2}$ interval as well as the $^6,7\text{Li}$ isotope shifts were determined with an uncertainty of 0.6 MHz, as listed in Tables 2 and 3.

The results for the $1\text{s}2\text{p } ^3\text{P}_{1-2}$ fine structure interval found by Rong et al. and Riis et al. strongly disagree, as shown in Table 2. This discrepancy was resolved by an experiment whose apparatus is illustrated in Fig. 1 [13]. This experiment has the advantage of requiring only a single laser that is electro-optically modulated to excite an ion beam (LIBEO). It does not rely on calibration of a Fabry–Perot etalon using an ultrastable reference laser. The ion or atomic beam is excited by a diode or dye laser that is passed through an elec-

Table 2. Comparison of experimental and theoretical fine structure results.

Interval	Experiment (MHz)	Technique (fm)	Theory (MHz)
${}^7\text{Li}^+ 1s2p \ 3P_{1-2}$	$62\ 667.4 \pm 2.0$	LH [10]	$62\ 679.4 \pm 0.5$ [14]
	$62\ 678.41 \pm 0.67$	LIB [11]	
	$62\ 679.46 \pm 0.98$	LIBEO [9]	
${}^6\text{Li} 2P$	$10\ 052.76 \pm 0.22$	LC [20]	$10\ 050.85 \pm 0.02 \pm 3$ [6]
	$10\ 050.2 \pm 1.5$	LAB [23]	
	$10\ 051.62 \pm 0.20$	LAB [25]	
	$10\ 053.044 \pm 0.091$	LABEO [17]	
	$10\ 052.964 \pm 0.050$	LABEO [27]	
	$10\ 052.862 \pm 0.067$	LAB [29]	
${}^7\text{Li} 2P$	$10\ 053.24 \pm 0.22$	LC [20]	$10\ 051.24 \pm 0.02 \pm 3$ [6]
	$10\ 053.184 \pm 0.058$	ODR [21]	
	$10\ 056.6 \pm 1.5$	LAB [23]	
	$10\ 053.2 \pm 1.5$	LAB [24]	
	$10\ 053.40 \pm 0.20$	LAB [25]	
	$10\ 052.37 \pm 0.11$	LAB [17]	
	$10\ 053.119 \pm 0.058$	LABEO [27]	
	$10\ 051.999 \pm 0.041$	LAB [29]	

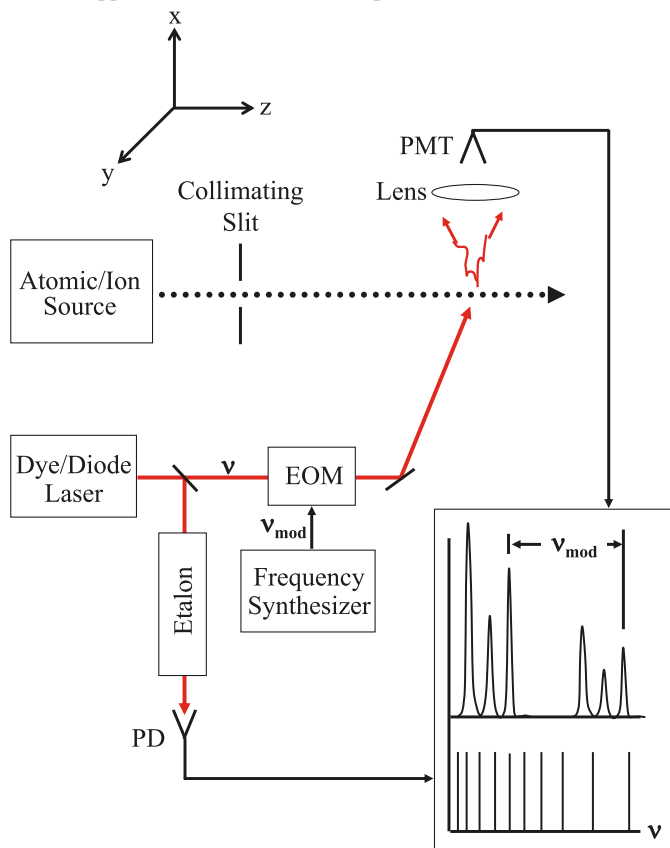
Note: The following abbreviations of the experimental techniques are described in the text: LH = laser heterodyne; LA(I)B = laser atomic (ion) beam; LC = level crossing; ODR = optical double resonance; LA(I)BEO = laser atomic (ion) beam using electrooptic modulation. The first uncertainty listed for the theoretical result is the calculational uncertainty, while the second number is the estimated effect of higher order terms not taken into account.

Table 3. Measured isotope shifts, field shifts, and determination of difference in mean-square nuclear charge radius.

Ref.	Transition	Isotope shift (MHz)	Field shift (MHz)	Δr^2 (fm ²)
LIB [11]	$\text{Li}^+ 2 \ 3S_1 \rightarrow 2 \ 3P_0$	$34,747.73 \pm 0.55$	7.56 ± 0.55	0.78 ± 0.06
	$\text{Li}^+ 2 \ 3S_1 \rightarrow 2 \ 3P_1$	$34,747.46 \pm 0.67$	7.59 ± 0.67	0.78 ± 0.07
	$\text{Li}^+ 2 \ 3S_1 \rightarrow 2 \ 3P_2$	$34,748.91 \pm 0.62$	6.20 ± 0.62	0.64 ± 0.06
FM [22]	D1 line	$10\ 532.9 \pm 0.6$	0.8 ± 0.6	0.32 ± 0.24
	D2 line	$10\ 533.3 \pm 0.5$	0.8 ± 0.5	0.32 ± 0.20
LAB [23]	D1 line	$10\ 534.3 \pm 0.3$	2.19 ± 0.3	0.89 ± 0.12
	D2 line	$10\ 539.9 \pm 1.2$	7.39 ± 1.2	3.01 ± 0.49
LAB [25]	D1 line	$10\ 533.13 \pm 0.15$	1.02 ± 0.15	0.41 ± 0.06
	D2 line	$10\ 534.93 \pm 0.15$	2.42 ± 0.15	0.99 ± 0.06
LABEO [17]	D1 line	$10\ 534.26 \pm 0.13$	2.15 ± 0.13	0.87 ± 0.05
LABEO [27]	D1 line	$10\ 534.039 \pm 0.070$	1.93 ± 0.07	0.78 ± 0.03
	D2 line	$10\ 534.194 \pm 0.104$	1.69 ± 0.10	0.69 ± 0.04
LAB [29]	D1 line	$10\ 354.215 \pm 0.039$	2.10 ± 0.04	0.86 ± 0.02
	D2 line	$10\ 533.352 \pm 0.068$	0.85 ± 0.07	0.34 ± 0.03
LAB [26]	D1 line	$10\ 533.160 \pm 0.068$	1.05 ± 0.07	0.43 ± 0.03
	$\text{Li} 2 \ 2S_{1/2} \rightarrow 3 \ 2S_{1/2}$	$11\ 453.734 \pm 0.030$	0.91 ± 0.03	0.58 ± 0.02
LAB [32]	$\text{Li} 2 \ 2S_{1/2} \rightarrow 3 \ 2S_{1/2}$	$11\ 453.95 \pm 0.13$	1.13 ± 0.13	0.72 ± 0.08
LAB [2]	$\text{Li} 2 \ 2S_{1/2} \rightarrow 3 \ 2S_{1/2}$	$11\ 453.984 \pm 0.020$	1.16 ± 0.02	0.74 ± 0.01

troptic modulator (EOM). The modulation frequency ν_{mod} is conveniently specified by a frequency synthesizer with an accuracy of three parts in 10^7 . Fluorescence, detected by a photomultiplier (PMT), is recorded as the laser frequency is scanned across the resonance. Each transition is excited by the various frequency sidebands of the modulated laser beam, enabling each laser scan to be calibrated. The linear-

ity of the laser scan is monitored by recording the transmission of part of the laser beam through an etalon using a photodiode (PD). The resulting fine structure measurement listed in Table 2 is in excellent agreement with that found by Riis et al. The average value of these two experimental results, $62\ 678.75 \pm 0.55$ MHz closely matches the theoretical estimate [14].

Fig. 1. Apparatus. See text for description.

2.2. Li D Lines

The transitions between the various hyperfine levels denoted by quantum number F comprising the lithium D lines are shown in Fig. 2. The energy levels were calculated using the most accurate hyperfine data available in the literature [15, 16]. The natural line width of the D lines derived from the lifetime of the 2P state is 5.8 MHz. This complicates the determination of the 2P fine structure splittings, as it is not possible to resolve the hyperfine levels of the ${}^6\text{Li } 2P_{3/2}$ state and only partially possible for the ${}^7\text{Li } 2P_{3/2}$ state.

One of the first high-precision determinations of the ${}^{6,7}\text{Li}$ 2P fine structure splitting was done using the level crossing (LC) technique [20]. Atoms were placed in a variable magnetic field and excited to the 2P state using linearly polarized light produced by an rf discharge lamp. A photomultiplier monitored the fluorescence emitted from the cell when the excited state radiatively decayed back to the ground state. Signals were obtained for the cases when fluorescence was linearly polarized parallel and perpendicular to the magnetic field. The splitting between the Zeeman sublevels became larger as the magnetic field was increased. At certain values of the magnetic field, the Zeeman sublevels of different fine structure levels were degenerate. This produced an interference effect that caused a change in the ratio of vertical to horizontal linearly polarized fluorescence.

The ${}^7\text{Li}$ 2P fine structure has also been studied using the optical double resonance (ODR) method [21]. Atoms were placed in a uniform magnetic field and excited using a lamp. A radio frequency was then applied to excite transi-

tions among the fine structure levels. Fluorescence, produced when the 2P state radiatively decayed to the ground state, was detected as a function of the radio frequency. A change in the intensity of circularly polarized fluorescence occurred when the radio frequency was resonant between the fine structure levels.

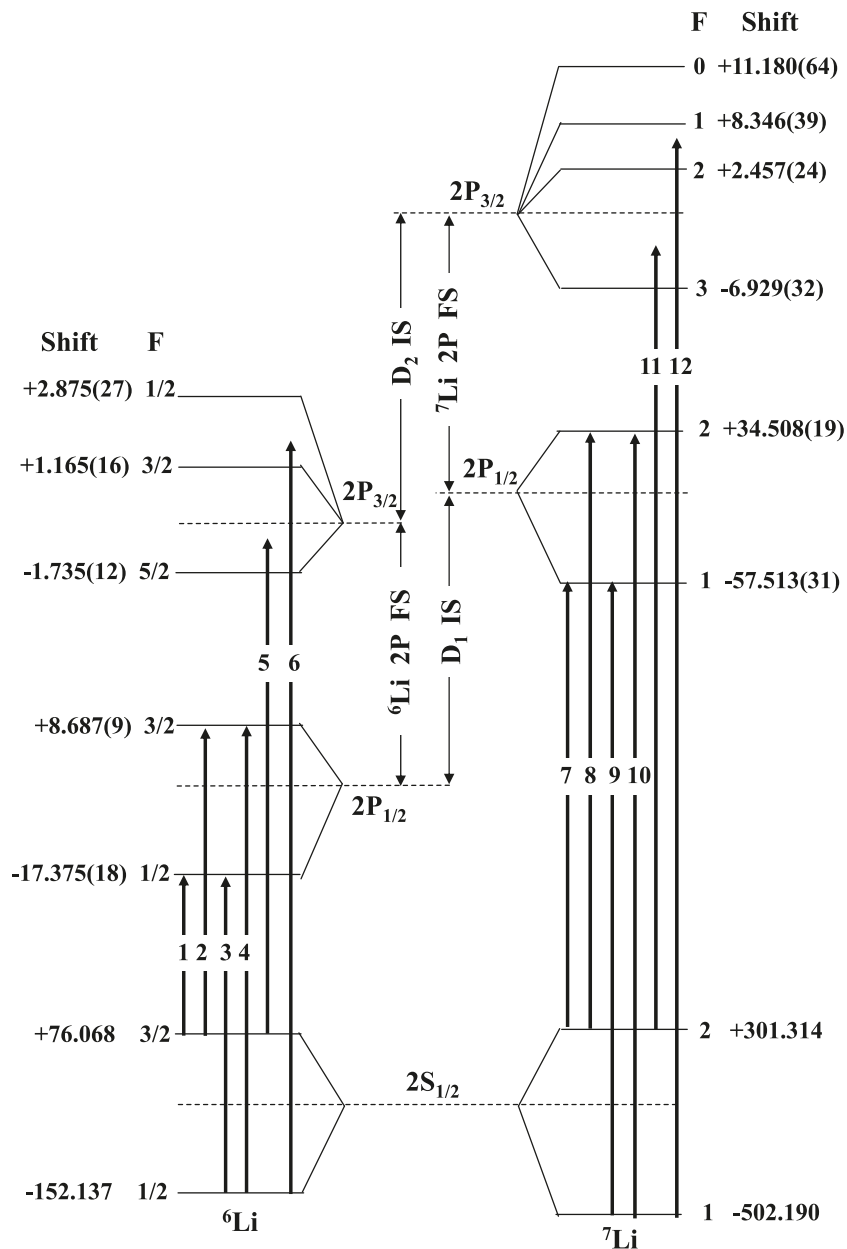
The ${}^{6,7}\text{Li}$ isotope shifts of the D1 and D2 lines have been found using Doppler free frequency modulation spectroscopy (FM) [22]. A saturated absorption signal was obtained using a weakly collimated atomic beam and a ring dye laser. Part of the laser beam was directed into a wavemeter to measure the absolute laser frequency. A Fabry-Perot marker etalon monitored the laser frequency as it was scanned. The remainder of the laser beam was split into pump and probe beams that counterpropagated through the lithium vapour cell. The probe beam passed through an electrooptic modulator creating sidebands containing 10% of the laser power at 20 MHz intervals around the central laser frequency. The sidebands probed the saturated absorption induced by the pump beam as the dye laser was scanned across a lithium resonance. The probe laser beam was attenuated when its frequency coincided with a lithium resonance. Part of the probe laser beam was focussed onto a fast photodiode to measure the amplitude and phase of the beating between the laser fundamental and its sidebands.

A number of measurements of fine structure and isotope shifts have been made using a laser to excite a collimated atomic beam (LAB) [23–26]. This generates much narrower spectral lines, which are limited by the transition natural line width instead of the much larger Doppler width observed in a cell. A typical atomic beam having a divergence of 1 mrad can be generated using a slit to collimate atoms emerging from an oven. A laser beam then intersects the atomic beam orthogonally to minimize Doppler broadening. Fluorescence is detected as the laser frequency is scanned across the resonance. The change in laser frequency is determined by passing part of the laser beam through a high-finesse etalon. A transmission peak occurs whenever the laser changes by an amount equal to the cavity free spectral range, which is inversely proportional to the etalon length. These experiments therefore rely on accurate calibration of the etalon, which usually is accomplished with a reference HeNe laser, whose frequency is locked using an iodine reference cell. The etalon is normally isolated in a vacuum chamber to minimize vibrations as well as fluctuations in temperature and pressure. However, multiple experiments performed by a group using the LAB technique have been in conflict, as is evident in Table 2, especially for the ${}^7\text{Li}$ 2P fine structure [23–25].

The problems associated with accurate etalon calibration can be avoided using an electro-optically modulated laser beam, as described in Section 2.1. Our first experiment excited the Li D lines using a diode laser [17]. Fluorescence was recorded on a digital oscilloscope as the laser was scanned across the resonance. The diode laser scan was linearized using the frequency markers obtained by passing part of the laser beam through an etalon. Figure 3a shows a sample signal obtained when the laser was scanned across the ${}^6\text{Li}$ D1 line.

A number of improvements were made in a subsequent experiment [27]. First, a ring dye laser was used because it had a 100 times smaller scan nonlinearity than the diode la-

Fig. 2. The energies of the hyperfine levels are in MHz with the uncertainties in brackets [18]. They were computed using the following values for the magnetic dipole a and electric quadrupole b constants. For ${}^6\text{Li}$: $a(2S_{1/2}) = 152.136\,840\,7$, $a(2P_{1/2}) = 17.375 \pm 0.018$, $a(2P_{3/2}) = -1.155 \pm 0.008$ and $b(2P_{3/2}) = -0.010 \pm 0.014$. For ${}^7\text{Li}$: $a(2S_{1/2}) = 401.752\,043\,3$, $a(2P_{1/2}) = 46.010 \pm 0.025$, $a(2P_{3/2}) = -3.055 \pm 0.014$ and $b(2P_{3/2}) = -0.221 \pm 0.029$.

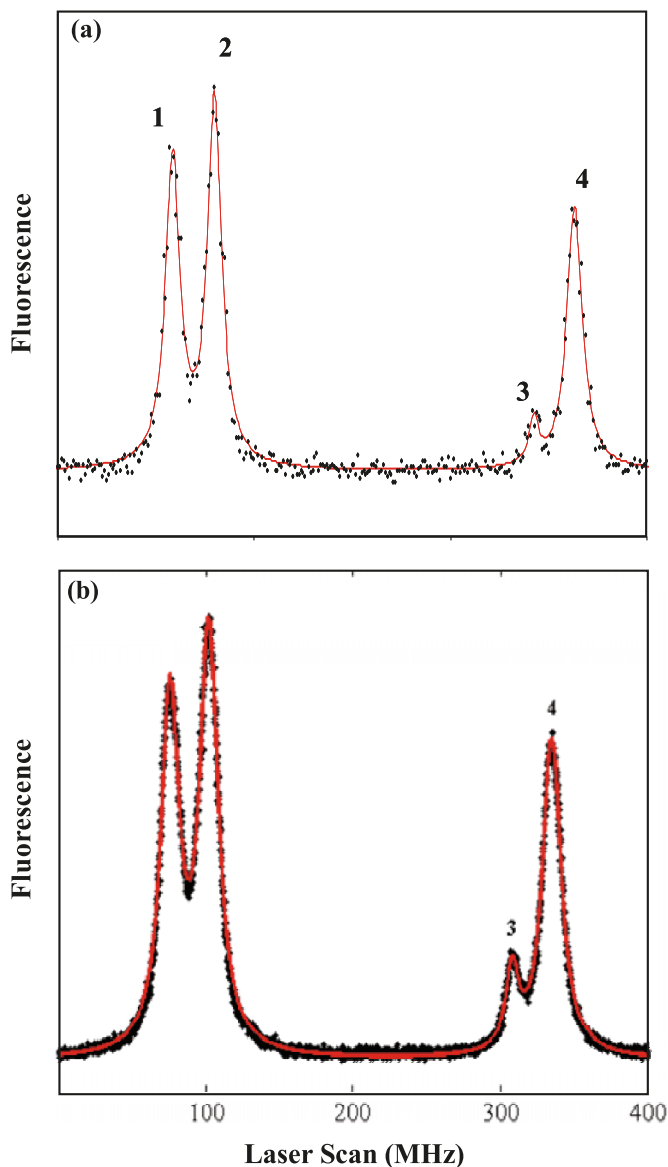


ser [27]. A longer etalon having a spectral range of 150 MHz monitored each laser scan. The residual magnetic field in the region where the laser and atomic beams intersect was also reduced to less than 20 mG using three pairs of Helmholtz coils. Finally, the data acquisition system was improved to record data every 12 kHz instead of every 1 MHz. The improved resolution is evident in Figs. 3 and 4. Both the initial and later experiments were tested by checking that the measured ${}^6,{}^7\text{Li}$ ground state hyperfine splittings agreed with the accepted atomic clock values [28].

The peaks shown in Figs. 3 and 4 were fitted to Lorentzian functions. The improvement in data sampling simplified the fitting of composite peaks, such as shown in Fig. 4.

Peaks 11 and 12 were fitted to three Lorentzian functions whose center frequencies were separated by the known hyperfine splittings of the ${}^7\text{Li } 2P_{3/2}$ state. Our initial experiment fixed the relative amplitudes of the three Lorentzians by estimating the contribution of each upper state hyperfine level to the resulting fluorescence signal. This can be naively estimated by considering the square of the Clebsch–Gordan coefficients for the respective transitions. This assumes that the ground-state hyperfine sublevels remain equally populated as the atom traverses the laser beam. However, an atom traveling at a thermal speed undergoes repeated excitation and radiative decay that alter the relative hyperfine sublevel populations. These optical pumping ef-

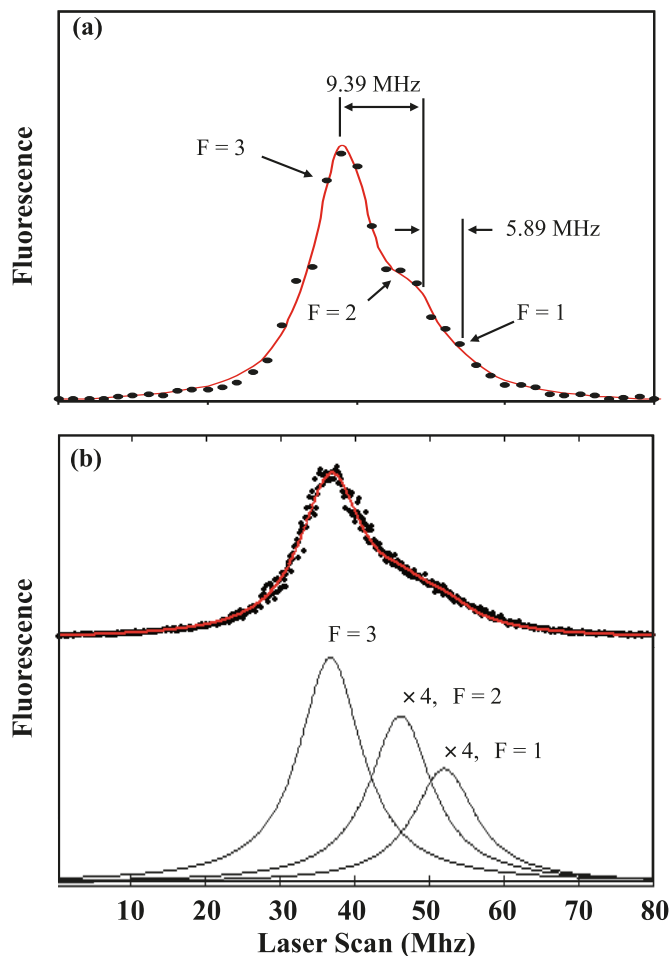
Fig. 3. Excitation of the ${}^6\text{Li}$ D1 Transition. Data was taken every (a) 1 MHz in our initial experiment and (b) 12 kHz in a later experiment. The peak numbers correspond to transitions labelled as shown in Fig. 2. The solid curve was fitted to the data as described in the text.



fects were taken into account in our original work to estimate the relative amplitudes of the three Lorentzians to peak 11. In our later experiment, peaks 11 and 12 were fitted by allowing the peak amplitudes to vary. The resulting observed amplitudes of the relative contributions of the upper state hyperfine levels to the fluorescence predicted by our model for peaks 11 and 12 agreed very closely with those found by the fitting program [27].

Tables 2 and 3 show the results obtained by the two experiments for the D1 isotope shift and the ${}^6\text{Li}$ 2P fine structure agree, although the later experiment has nearly twice the accuracy. The results for the ${}^7\text{Li}$ 2P fine structure disagree. Our initial experiment could only analyze peak 11, where the signal is dominated by fluorescence generated by the $2\text{P}_{3/2}$ $F = 3$ hyperfine level. The much improved resolu-

Fig. 4. Peak 11 observed in our initial (a) and later (b) experiments. This peak arises from excitation of the $2\text{S}_{1/2}$ $F = 2$ hyperfine level to the $2\text{P}_{3/2}$ $F = 1, 2, 3$ hyperfine levels. (b) Data were fitted to a summation of three Lorentzian functions shown at the bottom of the figure, two of which have been magnified by a factor of 4.



tion in the later experiment permitted the analysis of peak 12. The ${}^7\text{Li}$ 2P fine structure results that were found when analyzing peaks 11 and 12 were $10\,053.116 \pm 0.079$ and $10\,053.123 \pm 0.086$ MHz, respectively, which are in excellent agreement. These values were averaged to give the result listed in Table 2.

The most recent laser atomic beam experiment was performed using a diode laser [29]. The laser was locked to the lithium resonance and absolute transition frequencies of the ${}^6,{}^7\text{Li}$ D lines were determined. This was done by frequency shifting part of the diode laser beam by an AOM. The resulting laser beam was directed into an optical cavity, whose length was fixed using another diode laser that was locked to one of the hyperfine transitions in the D2 line of ${}^{87}\text{Rb}$ at 780 nm. The unknown diode laser frequency was found by measuring the AOM frequency required for the laser to be in resonance with the cavity and using the known wavelength of the Rb transition. The lithium peaks have a signal to noise ratio comparable to that shown in Figs. 3 and 4. The data analysis did not consider the effect of changing relative hyperfine sublevel populations as the atoms traversed the laser beam. It also appears that an incorrect value for

Table 4. Determination of rms ${}^6\text{Li}$ nuclear charge radius using $r({}^7\text{Li}) = 2.39 \pm 0.03$ fm.

Transition	Δr^2 (fm ²)	$r({}^6\text{Li})$ (fm)	Ref.
$\text{Li}^+ 2\ {}^3\text{S} \rightarrow 2\ {}^3\text{P}$	0.735 ± 0.036	2.539 ± 0.035	[11]
Li D lines	0.755 ± 0.023	2.543 ± 0.033	[27]
Li $2\text{S} \rightarrow 3\text{S}$	0.739 ± 0.013	2.540 ± 0.031	[2]
Average	0.742 ± 0.011	2.540 ± 0.031	
Electron scattering	0.79 ± 0.25	2.55 ± 0.04	[34]
Nuclear theory	0.74 ± 0.15	2.54 ± 0.01	[33]

the ${}^6\text{Li}$ $2\text{P}_{3/2}$ electric quadrupole constant was used to calculate the energies of the hyperfine levels [18]. The same apparatus has been used to measure the hyperfine splitting of the ${}^7\text{Li}$ $2\text{P}_{1/2}$ state [30]. The resulting magnetic dipole constant disagrees by 9σ from those found by other experimental and theoretical groups [31].

2.3. Li $2\ {}^2\text{S}_{1/2} \rightarrow 3\ {}^2\text{S}_{1/2}$ transition

This transition has been studied using two-photon Doppler free spectroscopy. The apparatus was developed at the GSI accelerator to first study the stable isotopes ${}^6,7\text{Li}$ [26] and subsequently the radioactive isotopes ${}^8,9\text{Li}$ [32]. It was later moved to the TRIUMF accelerator, which generated a high flux of ${}^{11}\text{Li}$ [2]. All the experiments were done in a weakly collimated atomic beam. The two-photon transition $2\ {}^2\text{S}_{1/2} \rightarrow 3\ {}^2\text{S}_{1/2}$ was excited using light produced by a titanium sapphire (TIS) ring laser operating at 735 nm. The upper state was then ionized using another laser beam. The ions were separated and detected using a quadrupole mass spectrometer. The ion signal was measured as a function of the TIS laser frequency with a resolution of approximately 1 MHz per channel. The resulting signal peaks were fitted using two Gaussian pedestals, corresponding to Doppler-broadened excitation of the background gas and the atomic beam, as well as a Voigt profile that described the Doppler free excitation. Each experiment was tested by measuring the magnetic dipole hyperfine constant of the Li $3\text{S}_{1/2}$ state and the $2\text{S} \rightarrow 3\text{S}$ transition energy. The results of these quantities agreed with theory as well as previous measurements but were an order of magnitude more accurate.

The initial experiment used a TIS laser that was frequency stabilized and scanned by offset locking to a single mode HeNe laser using an evacuated and temperature stabilized confocal interferometer [26]. The latter was calibrated using the ${}^{87}\text{Rb}$ ground-state hyperfine splitting observed in the $5\text{S} \rightarrow 5\text{D}$ two-photon excitation at 778 nm. The Li $3\text{S}_{1/2}$ state was ionized using an Ar^+ laser operating at 514 nm. The isotope shift for the $2\ {}^2\text{S}_{1/2} \rightarrow 3\ {}^2\text{S}_{1/2}$ transition, listed in Table 3, has a 30 kHz error that appears to be dominated by statistical uncertainty.

The experiment was refined to enhance the efficiency of ion detection to study the radioactive isotopes as well as ${}^6,7\text{Li}$ [32]. The TIS laser first excited the $2\text{S} \rightarrow 3\text{S}$ two-photon transition. The upper state spontaneously decays to the $2\ {}^2\text{P}_{1/2,3/2}$ states. A dye laser operating at 610 nm then excited the $2\text{P}_{3/2} \rightarrow 3\text{D}_{3/2,5/2}$ transition. This state was subsequently ionized by either the dye or TIS laser photons. Laser intensities of ~ 17 W/mm² were required to saturate the transitions. These intensities were attained by enclosing the interaction

region of the lasers with the lithium atoms in an optical cavity. This enhanced the laser power by a factor of 100. The resonator was locked to the TIS laser, while the dye laser was locked to the resonator. Efficient excitation occurred even though the dye laser was not tuned to the center frequency of the transition, because the resonance was power broadened. The TIS laser was stabilized by frequency offset locking to a reference diode laser that was in turn locked to an iodine line. A photodiode, having a 25 GHz bandwidth, detected the beat frequency between the TIS and diode lasers. An important systematic effect was that the beat frequency shifted as a function of the TIS laser power. Data were therefore taken at a variety of laser powers. The isotope shift, extrapolated to zero power listed in Table 3, has an uncertainty of 130 kHz which is dominated by this AC-Stark shift correction.

The most recent isotope shift measurement obtained at TRIUMF is listed in Table 3 [2]. It has an uncertainty of only 20 kHz, which is over six times smaller than that of their previous experiment [32]. No reason is given for this. Their latest result disagrees with their initial experiment by about 5 times the combined uncertainties. This discrepancy is attributed to unaccounted systematic error in the interferometric measurements of the original work.

3. Discussion and conclusions

Values for the field shifts and Δr^2 determined for the various transitions are listed in Table 3. For convenience, the data are listed separately for each experiment. The three results found by Riis et al. for the $\text{Li}^+ 2\ {}^3\text{S}_1 \rightarrow 2\ {}^3\text{P}_{0,1,2}$ transitions are mutually consistent. For the Li D lines, the two values of Δr^2 obtained using the frequency modulation (FM) technique agree but are substantially lower than those obtained by all other experiments. A number of laser atomic beam experiments (LAB) have yielded D1 and D2 isotope shifts that yield sharply conflicting values for Δr^2 . This indicates these experiments have been too optimistic in estimating their error. The experiment that used the LABEO technique yielded consistent results and their average is listed in Table 4. This method has the advantage of not relying on calibration of an interferometer, as is the case in the LAB experiments. For the Li $2\ {}^2\text{S}_{1/2} \rightarrow 3\ {}^2\text{S}_{1/2}$ transition, the last two results obtained by the GSI/TRIUMF group are consistent and were averaged to give the result listed in Table 4.

Table 4 shows that the values for Δr^2 found for the three transitions are in excellent agreement. This is particularly impressive since these results were determined using different experimental techniques. The average result for Δr^2 agrees with theory [33] as well as with the result of an electron scattering experiment but is 25 times more precise than the latter [34]. Table 4 also lists the resulting ${}^6\text{Li}$ nuclear charge radius found using the ${}^7\text{Li}$ nuclear charge radius determined using electron scattering 2.39 ± 0.03 fm [34].

Table 2 shows there is now agreement between the latest two experiments and the theoretical prediction for the fine structure splitting of the $\text{Li}^+ 1\text{s}2\text{p}\ {}^3\text{P}_{1-2}$ interval. However, considerable disagreement exists among experiments that used the LAB technique to determine the 2P fine structure. This is not surprising, since the same experiments have yielded inconsistent values for the field shift, as discussed

previously. It is therefore interesting to average the results for the 2P fine structure discarding the results of the LAB experiments. For ${}^6\text{Li}$, averaging the results of the LABEO and the LC experiments gives a value of $10\,052.954 \pm 0.049$ MHz. For ${}^7\text{Li}$, the result of Noble et al. [27] is consistent with those of the LC and ODR experiments. The average of these three results is $10\,053.154 \pm 0.040$ MHz. These results are about 2 MHz above theory, which did not take into account mass-independent higher order terms. Indeed, the theoretical results listed in Table 2 have a computational uncertainty as well as a 3 MHz uncertainty due to these higher order effects. Similar terms in two electron systems have been found to have a magnitude of several MHz [1]. Calculating the Li 2P fine structure therefore will be an important test of the Hylleraas variational method applied to a three electron system.

It has been pointed out that the so-called splitting isotope shift (SIS), which equals the difference of the ${}^6\text{Li}$ and ${}^7\text{Li}$ fine structure splittings, should be nearly independent of QED and nuclear volume effects [7]. Theory predicts a value for the SIS of 0.395 ± 0.006 MHz [7]. The result found using the 2P fine structure splittings, estimated in the preceding paragraph, is 0.200 ± 0.063 MHz. This is nearly 3 standard deviations below the theoretical result. Nevertheless, this is much closer than that found by the latest LAB experiment that yields inconsistent results for Δr^2 [29]. Their result for SIS, -0.863 ± 0.079 MHz, disagrees from theory by nearly 16σ .

In conclusion, a number of experiments have measured isotope shifts using the LAB experimental method and have encountered problems calibrating interferometers. In the future, absolute transition frequency measurements will undoubtedly be improved using the femtosecond frequency comb technique [35]. However, the determination of the Li 2P fine structure will be limited by the accuracy of the hyperfine splittings of the ${}^6,7\text{Li}$ $2P_{3/2}$ states. It will be difficult to improve the magnetic dipole and electric quadrupole constants of this state, as the D2 transition line width is comparable to the hyperfine splittings. An important test of experimental results is to check whether the values for the difference in mean-square nuclear charge radius obtained by measuring isotope shifts of different transitions are consistent. Experiments passing this test and studying three different optical transitions yield data in excellent agreement. The combination of precise Hylleraas variational calculations plus high-resolution optical spectroscopy can now reliably determine relative nuclear sizes with millifermi accuracy.

4. Acknowledgements

The authors wish to thank the Canadian Natural Science and Engineering Research Council for financial support. GN is the recipient of an Ontario Graduate Scholarship in Science and Technology.

References

1. G.W.F. Drake, W. Nörtershäuser, and Z.C. Yan. *Can. J. Phys.* **83**, 311 (2005). doi:10.1139/p05-020.
2. R. Sánchez, W. Nörtershäuser, G. Ewald, D. Albers, J. Behr, P. Bricault, B.A. Bushaw, A. Dax, J. Dilling, M. Dombisky, G.W.F. Drake, S. Götze, R. Krichner, H.-J. Kluge, T. Kühl, J. Lassen, C.D.P. Levy, M.R. Pearson, E.J. Prime, V. Ryjkov, A.

- Wojtaszek, Z.C. Yan, and C. Zimmerman. *Phys. Rev. Lett.* **96**, 033002 (2006). doi:10.1103/PhysRevLett.96.033002.
3. W.A. van Wijngaarden. *Can. J. Phys.* **83**, 327 (2005). doi:10.1139/p05-010.
4. W.A. van Wijngaarden and G.A. Noble. *Lect. Notes Phys.* **745**, 111 (2008). doi:10.1007/978-3-540-75479-4_7.
5. G.W.F. Drake. *In Atomic, Molecular and Optical Physics Handbook. Edited by G. W. F. Drake.* AIP, New York, USA, 1996.
6. Z.C. Yan and G.W.F. Drake. *Phys. Rev. A*, **66**, 042504 (2002). doi:10.1103/PhysRevA.66.042504.
7. Z.C. Yan, W. Nörtershäuser, and G.W.F. Drake. *Phys. Rev. Lett.* **100**, 243002 (2008). doi:10.1103/PhysRevLett.100.243002.
8. M. Puchalski, A.M. Moro, and K. Pachucki. *Phys. Rev. Lett.* **97**, 133001 (2006). doi:10.1103/PhysRevLett.97.133001.
9. J.J. Clarke and W.A. van Wijngaarden. *Phys. Rev. A*, **67**, 012506 (2003). doi:10.1103/PhysRevA.67.012506.
10. H. Rong, S. Grafström, J. Kowalski, G. zu Putlitz, W. Jastrzebski, and R. Neumann. *Z. Phys. D At. Mol. Clust.*, **25**, 337 (1993). doi:10.1007/BF01437300.
11. E. Riis, A.G. Sinclair, O. Poulsen, G.W.F. Drake, W.R.C. Rowley, and A.P. Levick. *Phys. Rev. A*, **49**, 207 (1994). doi:10.1103/PhysRevA.49.207.
12. W. Demtröder. *In Laser Spectroscopy.* Springer-Verlag, New York, USA, 1988.
13. W.A. van Wijngaarden. *Adv. At. Mol. Opt. Phys.* **36**, 141 (1996).
14. T. Zhang, Z.C. Yan, and G.W.F. Drake. *Phys. Rev. Lett.* **77**, 1715 (1996). doi:10.1103/PhysRevLett.77.1715.
15. E. Arimondo, M. Inguscio, and P. Violino. *Rev. Mod. Phys.* **49**, 31 (1977). doi:10.1103/RevModPhys.49.31.
16. [The magnetic dipole hyperfine constant $a({}^7\text{Li } 2P_{1/2})$ has been determined to be 45.914 ± 0.025 by Orth et al. as well as 46.010 ± 0.025 [17] and 45.893 ± 0.026 MHz in our two experiments. The energies of the $2P_{1/2}$ hyperfine levels are $E_{F=2} = 0.375a$ and $E_{F=1} = 0.625a$. The 2P fine structure and D1 isotope shift are defined relative to the $2P_{1/2}$ center of gravity. This can be found without using the hyperfine splitting of either the upper or lower state by using linear combinations of the frequencies of the transitions labelled 7 to 10 in Fig. 2].
17. J. Walls, R. Ashby, J.J. Clarke, B. Lu, and W.A. van Wijngaarden. *Eur. Phys. J. D*, **22**, 159 (2003).
18. [Arimondo et al. lists two different values, -0.010 ± 0.014 and -0.10 ± 0.14 MHz for $b({}^6\text{Li } 2P_{3/2})$ as well as $b({}^7\text{Li } 2P_{3/2}) = -0.221 \pm 0.029$ MHz. The ratio of the ${}^6\text{Li}$ and ${}^7\text{Li}$ electric quadrupole constants should equal the ratio of the nuclear electric quadrupole moments whose magnitude has been found to be 0.023. Hence, the correct value for $b({}^6\text{Li } 2P_{3/2})$ is -0.010 ± 0.014 MHz].
19. N.A. Schuster and G.E. Pake. *Phys. Rev.* **81**, 157 (1951). doi:10.1103/PhysRev.81.157.
20. K.C. Brog, T.G. Eck, and H. Wieder. *Phys. Rev.* **153**, 91 (1967). doi:10.1103/PhysRev.153.91.
21. H. Orth, H. Ackermann, and E.W. Otten. *Z. Phys. A*, **273**, 221 (1975). doi:10.1007/BF01410002.
22. C.J. Sansonetti, B. Richou, J.R. Engleman, and L.J. Radziemski. *Phys. Rev. A*, **52**, 2682 (1995). doi:10.1103/PhysRevA.52.2682.
23. L. Windholz, H. Jäger, M. Musso, and G. Zerza. *Z. Phys. D At. Mol. Clust.* **16**, 41 (1990). doi:10.1007/BF01831564.
24. C. Umfer, L. Windholz, and M. Musso. *Z. Phys. D At. Mol. Clust.* **25**, 23 (1992). doi:10.1007/BF01437516.

25. W. Scherf, O. Khait, H. Jäger, and L. Windholz. *Z. Phys. D At. Mol. Clust.* **36**, 31 (1996). doi:10.1007/BF01437417.
26. B.A. Bushaw, W. Nörtershäuser, G. Ewald, A. Dax, and G.W.F. Drake. *Phys. Rev. Lett.* **91**, 043004 (2003). doi:10.1103/PhysRevLett.91.043004.
27. G.A. Noble, B.E. Schultz, H. Ming, and W.A. van Wijngaarden. *Phys. Rev. A*, **74**, 012502 (2006). doi:10.1103/PhysRevA.74.012502.
28. A. Beckmann, K.D. Boklen, and D. Elke. *Z. Phys.* **270**, 173 (1974). doi:10.1007/BF01680407.
29. D. Das and V. Natarajan. *Phys. Rev. A*, **75**, 052508 (2007). doi:10.1103/PhysRevA.75.052508.
30. D. Das and V. Natarajan. *J. Phys. B*, **41**, 035001 (2008). doi:10.1088/0953-4075/41/3/035001.
31. K. Beloy and A. Derevianko. *Phys. Rev. A*, **78**, 032519 (2008). doi:10.1103/PhysRevA.78.032519.
32. (a) G. Ewald, W. Nörtershäuser, A. Dax, S. Götte, R. Kirchner, H.-J. Kluge, T. Kühl, R. Sanchez, A. Wojtaszek, B.A. Bushaw, G.W.F. Drake, Z.C. Yan, and C. Zimmerman. *Phys. Rev. Lett.* **93**, 113002 (2004). doi:10.1103/PhysRevLett.93.113002.; (b) G. Ewald, W. Nörtershäuser, A. Dax, S. Götte, R. Kirchner, H.-J. Kluge, T. Kühl, R. Sanchez, A. Wojtaszek, B.A. Bushaw, G.W.F. Drake, Z.C. Yan, and C. Zimmerman. *Phys. Rev. Lett.* **94**, 039901 (2005). doi:10.1103/PhysRevLett.94.039901.
33. S.C. Pieper and R.B. Wiringa. *Annu. Rev. Nucl. Part. Sci.* **51**, 53 (2001). doi:10.1146/annurev.nucl.51.101701.132506.
34. C.W. de Jager, H. de Vries, and C. de Vries. *At. Nucl. Data Tables (N.Y.)*, **36**, 495 (1987). doi:10.1016/0092-640X(87)90013-1.
35. C.E. Simien, J.D. Gillaspay, and C.J. Sansonetti. ICAP Poster, (2008).